Theor Chem Account (2008) 120:447–457
DOI 10.1007/s00214-008-0421-z

REGULAR ARTICLE

Competition between Bailar and Ray-Dutt paths in conformational interconversion of tris-chelated complexes: a DFT study

Mario Amati · Francesco Lelj

Received: 15 November 2007 / Accepted: 5 February 2008 / Published online: 29 February 2008

Abstract Tris-chelated complexes of aluminum with α-isopropenyltropolonate and α-isopropyltropolonate ligands can be considered prototypical complexes for the study of internal rearrangements through prismatic transient structures. Such isomerization paths, known as Bailar and Ray-Dutt twists, have been suggested for these compounds on the basis of dynamic NMR study, but modern computational methodologies have never been applied to corroborate this finding. In this paper, we report a computational investigation about the internal isomerization processes of the mentioned complexes. Both the Bailar and Ray-Dutt twists have been found as possible reaction paths. The prismatic structures along each reaction path have been described as transition structures rather than intermediate and have been computationally characterized. A comparison between experimental and computational kinetic data has been performed.

Keywords Bailar twist · Ray-Dutt twist · Isomerizations · DFT · ONIOM · Tris-chelated complexes

1 Introduction

The discovery of the first tris-chelated metal complex with a prismatic geometry in 1965 [1] catalysed a lot of research works on this type of metal complexes. Till then, all the 6-coordinated metal complexes in their stable forms were assumed to be octahedral structures after the historical work of Werner [2]. Once the new structure was reported, many new tris-chelated complexes were produced and their crystallographic structures were determined with the aim to understand the chelant characteristics able to induce the prismatic geometry (Ref. [3] and references therein).

Indeed, the achievement of prismatic geometries was suggested as intermediate or transient structures along isomerization paths known as Bailar [4] and Ray-Dutt [5] twists. Figure 1 shows the characteristics of such twist processes in tris-chelated complexes. They consist in the rotation of one of the triangular faces of the octahedron respective to the opposite triangular face. During such a motion, an eclipsed configuration is reached which corresponds to a perfectly trigonal prismatic geometry of the coordination sphere. If the motion of the front face goes on, a new octahedral geometry is produced which is the mirror image of the starting one. Thus, a $\Lambda - \Delta$ inversion has occurred. The difference between the Bailar and Ray-Dutt twists is the relative position of the chelants in the prismatic geometry (Figs. 1a, b). In the case of the Bailar twist, the rotation takes place around the C_3 symmetry axis of the idealised D_3 point symmetry octahedral structure. As a consequence, the transient prismatic structure shows three parallel chelants and is referred to as trigonal prismatic structure. Besides, in the case of the Ray-Dutt twist, the rotation is pivoted by one of the perpendicular C_2 axis of the initial structure and the transient prismatic structure presents only two parallel chelants (rhombic prismatic structure).

A possible choice of the reaction coordinate for a twist rearrangement is the twist angle (Fig. 1c). It amounts to 60° for a perfectly octahedral geometry and 0° for a perfectly prismatic one. It is reasonable to predict that a 6-coordinated

This work is dedicated to the 60th birthday of Prof. Nino Russo.

Contribution to the Nino Russo Special Issue.

M. Amati · F. Lelj (✉)
INSTM sez. Basilicata and LaMI, Dipartimento di Chimica,
Università degli Studi della Basilicata, LASCAMM,
Via N. Sauro, 85, 85100 Potenza, Italy
e-mail: francesco.lelj@unibas.it

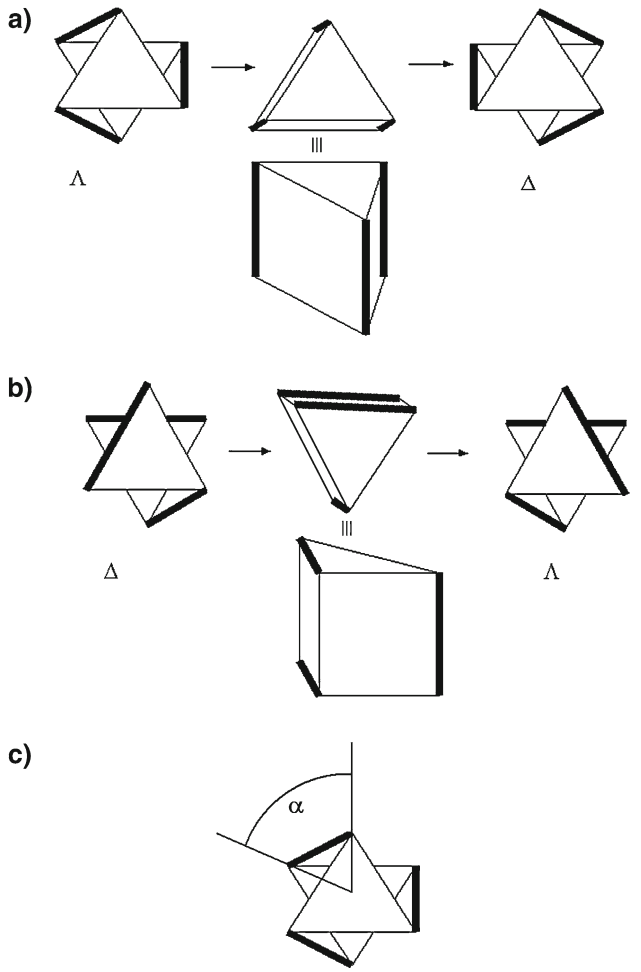

Fig. 1 **a** The Bailar twist process in the case of a tris-chelated metal complex of a symmetric chelant; **b** the Ray-Dutt twist process; **c** the definition of the twist angle, the rotation angle of one triangular face with respect to the opposite triangular face

compound whose structure is substantially distorted from the perfectly-octahedral geometry toward a prismatic geometry (that is with a twist angle significantly lower than 60°) is more suitable to invert its chirality by twist processes. In this light, particular importance assumes the work of Kepert [3], who rationalized many reported crystallographic structures of tris-chelated complexes. Interestingly, Kepert found that the twist angle of the ground state geometry in this class of complexes can be directly associated to the normalized bite of the chelant, that is the ratio of the distance between the two donor atoms in the same chelant and the metal-to-donor bond distance. The shorter is the normalized bite, the smaller is the twist angle. Furthermore, a simple model was introduced which was surprisingly capable of predicting the complex twist angle from the value of the normalized bite. On this basis, fast twist processes were postulated for tris-chelated complexes of short normalized bite. Additionally, the Bailar twist was predicted faster than the Ray-Dutt twist when the normalized bite is lower than 1.3.

The likelihood of twist processes and the preference for Bailar or Ray-Dutt twists was studied by Rodger and Johnson about 10 years later [6]. As in the Kepert's approach [3], great importance was assigned to the chelant structure. Also in this case, the authors concluded that short bite distances (and thus short normalized bites) should favour the Bailar twist.

The correspondence between small bite distances, small ground state twist angle and fast twist rate met many experimental confirmations. Pignolet et al. [7] pointed out a correlation between the Bailar twist rate and the high spin character in tris-chelated transition metal complexes. High spin complexes normally show longer bond distances and, consequently, smaller normalized bites. Such observations were corroborated by Healy and White [8], who reported smaller twist angles for high spin transition metal complexes. The $Co(Et, Et\text{-}dtc)_3$[1] [9,10] and $Co(acac)_3$ [11] present normalized bites of 1.23 and 1.50, respectively, and twist angles of 43.6° and 60°. It was found that the second compound probably undertakes isomerization processes through bond-breaking paths, as observed in other tris-chelated complexes of long bite distances [12,13]. The fact that $Co(acac)_3$ gives rise to isomerization processes through bond-breaking paths has been recently corroborated by ab initio computations [14].

However, some authors suggested that, in some transition metal complexes, the role of the central metal might be relevant. $Fe(phen)_3^{2+}$ is a low-spin complex in a singlet ground state and shows an activation enthalpy of about 29 kcal/mol for the Bailar twist [15]. On the other hand, the high-spin quintet $Fe(dtc)_2(phen)$ presents an activation enthalpy for the same process lower than 7.5 kcal/mol [7]. Such a noticeable difference was interpreted by the ligand field approach [16]. Low-spin d^6 complexes are particularly hindered in their twist motion in comparison to high-spin analogues by virtue of the higher destabilization of the ligand field. A confirmation of this point comes from the observed photoinduced $\Lambda - \Delta$ chirality inversion of $Cr(S\text{-}trp)_3$ [17]. This process is consistent with a Bailar twist which takes place after population of a d–d excited state. It confirms the importance of populating high energy d^* orbitals for faster twist mechanisms in transition metal complexes.

The group 13 Al(III), Ga(III) and In(III) complexes obviously do not present the electronic contribution induced by the ligand field destabilisation. In this case, the assumed Bailar twist rate follows the order Al(III)<Ga(III)<In(III) [18,19] in complexes with low bite distance chelants. Such

[1] Abbreviations for ligands used throughout: dtc = dithiocarbamato; Et,Et-dtc = N,N-diethyldithiocarbammate; phen = 1, 10-phenantroline; acac = acetylacetonate; S-trp = (s)-tryptophanato; T = tropolonate; α-C_3H_5-T = α-isopropenyltropolonate; α-C_3H_7-T = α-isopropyltropolonate.

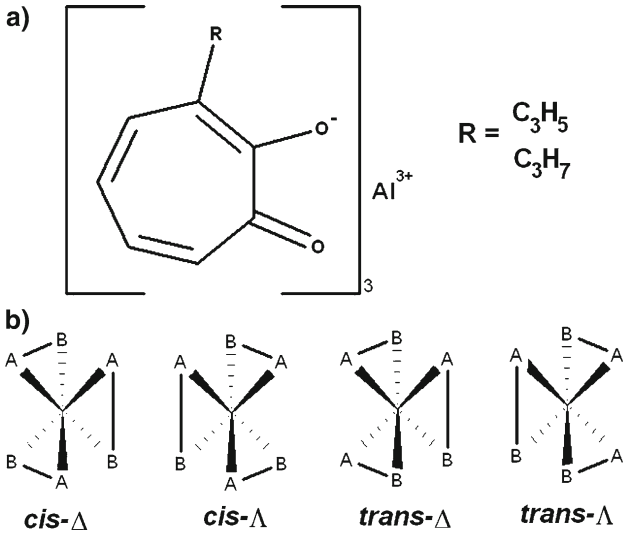

Fig. 2 **a** aluminum tris(α-isopropyltropolonate) and aluminum tris(α-isopropenyltropolonate) (Al(α-C_3H_7-T)$_3$ and Al(α-C_3H_5-T)$_3$); **b** the four isomers of tris-chelated complexes with an asymmetric ligand

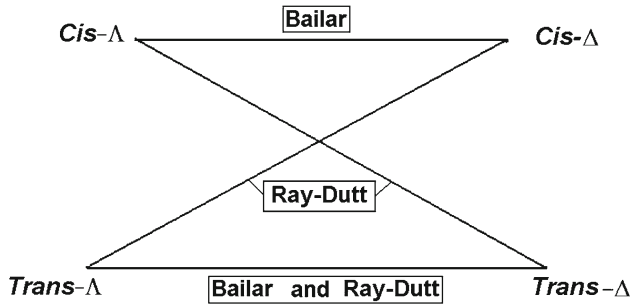

Fig. 3 The effects of the Bailar and Ray-Dutt twists on the stereoisomers of tris-chelated complexes with asymmetric chelants; the Bailar twist only inverts the structure chirality ($\Lambda - \Delta$ inversion), the Ray-Dutt twist from a *cis* structure additionally induces *cis–trans* isomerization ($\Lambda - \Delta$ inversion plus *cis–trans* isomerization). Three Ray-Dutt twists can take place from a *trans* structure: one of them leads to the *cis* structure ($\Lambda - \Delta$ inversion plus *cis–trans* isomerization), the other two ones only induce $\Lambda - \Delta$ inversion

a trend is compatible with the longer metal–donor bond distance and lower normalised bite. On the other hand, the same metal complexes do not clearly show twist processes when the ligands are β-diketonates [20], which presents a higher bite and possible dissociative isomerizations.

A particularly important evidence of twist processes was obtained by Holm et al. in studying tris(α-isopropyl-tropolonate) and tris(α-isopropenyl-tropolonate) metal complexes [21] (Fig. 2). They will be called Al(α-C_3H_5-T)$_3$ and Al(α-C_3H_7-T)$_3$ in the following. The presence of the hydrocarbon substituents on the tropolonate skeleton was a necessary request for the NMR study of the isomerization kinetics. The substituents make the chelant asymmetric. As a consequence, the number of minimum structures of the complex is doubled in comparison to the case of the symmetric chelant in aluminum tris(tropolonate) (AlT_3) (Fig. 1 for a graphical description of the Λ- and Δ-tris-chelated complexes with a symmetric chelant). From the two specular Λ- and Δ–AlT_3 isomers we pass to four isomers which consists in two couples of enanthiomeric structures, each couple is called *trans* and *cis* (Fig. 2). The *trans* isomers present two identical donor atoms in *trans* relative position (for example, in our complexes, the two oxygen atoms closer to the hydrocarbonic substituent). The *cis* isomers present all the identical donor atoms on the same triangular face of the octahedron. Nevertheless, the presence of four minima points connected by the isomerization minimum energy paths (MEPs) results into an increased complexity in the interpretation of the experimental data. Figure 3 shows the effects of the Bailar and Ray-Dutt twists in terms of chirality inversion and/or *cis-trans* isomerization.

In the work in object [21], the authors recognized low-temperature-induced (low activation) paths and high-temperature-induced (high activation) paths. The first ones consist in $\Lambda - \Delta$ chirality inversion without *cis–trans* isomerization. They were assigned to the Bailar twist of the *trans* isomer in Al(α-C_3H_5-T)$_3$. On the other hand, in Al(α-C_3H_7-T)$_3$, the $\Lambda - \Delta$ inversion was observed for both *cis* and *trans* isomers. The high temperature processes lead to *cis–trans* isomerization and were not assigned to any reaction path by the authors. The presence of a negative activation entropy was considered a distinctive character of the twist reaction paths. In fact, bond-breaking processes are supposed to be associated with positive and larger activation entropies.

The clear assignment of the collected NMR data on Al(α-C_3H_5-T)$_3$ and Al(α-C_3H_7-T)$_3$ to twist processes and the reported experimental activation parameters make this complexes good candidates for the application of modern computational techniques to the description of the twist processes. In this light, a recent computational approach based on the density functional theory [14] produced a good agreement with various experimental evidences of twist processes in M(acac)$_3$ complexes.

In this paper we report a computational investigation based on ab–initio techniques about the quickest isomerization processes of AlT_3, Al(α-C_3H_5-T)$_3$ and Al(α-C_3H_7-T)$_3$.

2 Methods

All the calculations were performed using the Gaussian03 program, revision B.05 [22]. Figures 5 and 6 have been produced by using the Molden program [23].

Molecular structures were optimized using the Kohn–Sham density functional theory (DFT) [24] with the Becke's three-parameters hybrid exchange-correlation functional

known as B3LYP [25] and the PBE functional of Pedew, Burke and Ernzerhof [26,27]. Several basis sets have been applied, as reported in the text, the most used ones were the 3-21G(d), the 6-31G(d) and the 6-311G(d,p). In all the cases, the standard basis sets of the Gaussian03 program have been applied. All the optimized geometries have been obtained using the standard threshold for SCF and geometry optimization. Analytical evaluation of the energy second derivative matrix w.r.t. Cartesian coordinates (Hessian matrix) at the same level of approximation confirmed the nature of minima and transition structures of the energy surface points associated to the optimized structures. The harmonic vibrations allowed the evaluation of zero-point corrections and the thermodynamic properties: enthalpy, Gibbs energies and entropy. All the computations have been performed using the Gaussian03 standard approach[2] which considers the molecule in a vacuum.

Two-layer ONIOM computations [28] have been performed by treating the C_3H_5 and C_3H_7 substituents on the tropolonate ligands at the semiempirical PM3 [29,30] level of approximation, and the rest of the molecule at the B3LYP/6-31G(d) level of approximation. Hydrogen atoms have been chosen as link-atoms between the two layers.

Solvation effects have been included by by the IEF-PCM method (integral equation formalism polarizable continuum model) [31]. Single point energy computations have been performed at the B3LYP/6-311G(d,p) level of approximation on the B3LYP/6-31G(d) optimized structures (no solvation effects for the optimized geometries). CH_2Cl_2 solvent has been chosen, and treated as parameterized in the Gaussian03 program.

All the reported computations have been performed in the closed-shell approximation, thus, all the computed electronic states are totally symmetric singlet states. The T_1 (lowest-in-energy triplet state) potential energy surface (PES) has been computed in each of the stationary points of the S_1 (ground state) PES. The lowest found energy difference between S_1 and T_1 has been 62 kcal/mol. Such a value rules out crossings between the two surfaces in all the studied reaction paths.

Fragment analysis of AlT3 (metal–ligand covalent interaction) has been performed with the ADF2000 [32] program using the BLYP xc functional (Becke's 1988 exchange [33] and correlation of Lee, Yang and Parr [34]) and double-zeta STO basis set plus one polarisation function on each atom (ADF set III).[3]

3 Results

The PES of AlT_3 has been computed with the aim to characterize its stationary points of interest. The primary interest has been addressed to the lowest-in-energy saddle points of order one (transition structures) which connect the minima points of interest.

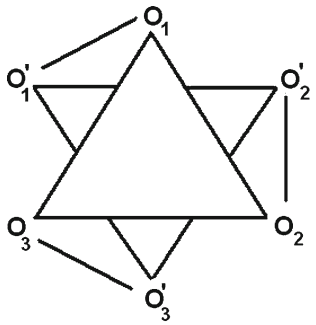

Fig. 4 AlT_3 donor atoms labels to be used in Table 1

Our report starts with the results obtained for AlT_3. The reason of this choice has been the presence of an experimentally obtained structure for this compound and the fact that only a low perturbation could be induced by the tropolonate substituents in $Al(\alpha\text{-}C_3H_5\text{-}T)_3$ and $Al(\alpha\text{-}C_3H_7\text{-}T)_3$ with consequent low influences on the PES. Additionally, the higher symmetry of AlT_3 allowed the application of symmetry rules [35–38] for the prediction of the symmetry point group of the transition structures.

3.1 Minima points of AlT_3

The minimum energy structure has been searched without symmetry constrains. The found structure belongs to the D_3 point group symmetry. Table 1 lists some geometrical parameter of the structure in comparison to the experimental ones [39] (Fig. 4 for the chosen labels of the donor atoms). In the analysed crystal, the molecule symmetry is lower (C_{2v}), possibly due to crystal packing forces. Thus, averaged parameters have been included in Table 1 that are referred to an idealised D_3 point group.

From Table 1, even though all the distances of the coordination sphere around the aluminium atom have been overestimated by the computations at the B3LYP/3-21G(d) and B3LYP/6-31G(d) levels of approximation, the normalised bite (ratio of the O–O distance on the same chelant and the Al–O bond distance) is well predicted by the computations and the coordination sphere twist angles are well reproduced.

The structure of the chelant (not reported in Table 1) is described with higher accuracy by both the used basis sets.

For the purposes of this manuscript, the prediction of the coordination sphere structure is particularly important. In this sense, the choice of the basis set should be addressed to a correct modelling of this part of the molecule. However, a mere comparison between the solid state experimental and computed geometrical parameters could not be a proper way to test the computational accuracy. In fact, packing effects

[2] http://www.gaussian.com/g_whitepap/thermo.htm.

[3] Available at http://www.scm.com/Doc/Doc2000/atomicdata/.

Table 1 Some computed geometrical parameters of AlT_3 in comparison to the experimental structure [35]. Fig. 4 for the atomic labels used

Parameter	B3LYP/3-21G(d) (Å and degrees)	B3LYP/6-31G(d) (Å and degrees)	Experimental [35] (Å and degrees)
Al–O	1.899	1.914	1.888 (2)
O1–O1' (Bite)	2.504	2.512	2.490 (6)
Normalised Bite	1.319	1.312	1.319 (3)
O1–O2	2.738	2.754	2.698 (26)
O1–O2'	2.766	2.814	2.797 (18)
C–O	1.311	1.286	1.291 (1)
O1–Al-O3'	172.4	171.2	170.9 (16)
O1–Al-O1'	82.5	82.0	82.6 (4)
O1–Al-O2	92.2	92.0	91.2 (11)
O1–Al-O2'	93.5	94.6	95.60 (9)
Twist angle	50.8	49.5	48.1 (13)

Table 2 A test of the performances of different basis sets in predicting important geometrical parameters of AlT_3

Basis set	Al–O distance (Å) (experimental [35] = 1.888 Å)	C–O distance (Å) (experimental [35] = 1.291 Å)
3-21G	1.904	1.309
3-21G(d)	1.899	1.311
6-31G	1.939	1.313
6-311G	1.937	1.312
6-31G(d)	1.914	1.286
6-311G(d,p)	1.915	1.281

could be able to change the Al–O distance of a significant amount because of the relatively low force constant of such bonds. It seems reasonable that packing effects shorten the chelant–metal distance in comparison to gas phase and solution phases as well.

Table 2 collects some results from full geometry optimizations performed with several basis sets. From a comparison between the 6-311G and 6-31G basis sets, it appears that the triple-zeta basis set does not lead to any improvement in comparison to the experimental measure. This fact is confirmed by the comparison between the 6-311G(d,p) basis set and the 6-31G(d). Comparing the 6-31G(d) and 6-31G basis sets allows to conclude that (not surprisingly) the polarization functions are more important than the use of triple-zeta basis sets. The fact that the 3-21G(d) basis set gives better results than the 6-31G(d) and larger basis sets is probably associated to basis set superimposition errors and lower angular flexibility of the basis set on the carbon and oxygen atoms (where the polarization functions are not present) that cause the shortening of the Al–O bond distance. From above, the determination of the transition structure has been limited to the 6-31G(d) basis set, which is the best compromise between computational effort and basis set superimposition error. Single point energy computations on the 6-31G(d) structures have been performed at the 6-311G(d,p) level for a correction of the electronic energy.

Figure 5 gives information about the Kohn–Sham orbitals of the isolated chelant fragment that are mostly involved in charge-transfer processes between the chelants and the central metal. Such computations have been performed using the ADF2000 program (see the Sect. 2 details). Only the four orbitals which are the highest-in-energy occupied orbitals in the isolated chelant and the two lowest-in-energy virtual fragment orbitals show deviations from the not-interacting electronic populations of 2.00 and 0.00 (respectively for occupied and virtual orbitals).

3.2 Transition structures of AlT_3

According to predictive approaches which postulate the existence of maximum symmetry reaction paths [40], two chiral PES minima points of D_3 symmetry, related by the application of a point reflection, should be connected by a MEP which passes through a transition structure of D_{3h} point symmetry. Such a structure has been effectively found and shown in Fig. 6a. The transition structure has been labelled as "TS-Bailar". The existence of this structure does not rule out the presence of lower symmetry transition structures that can be

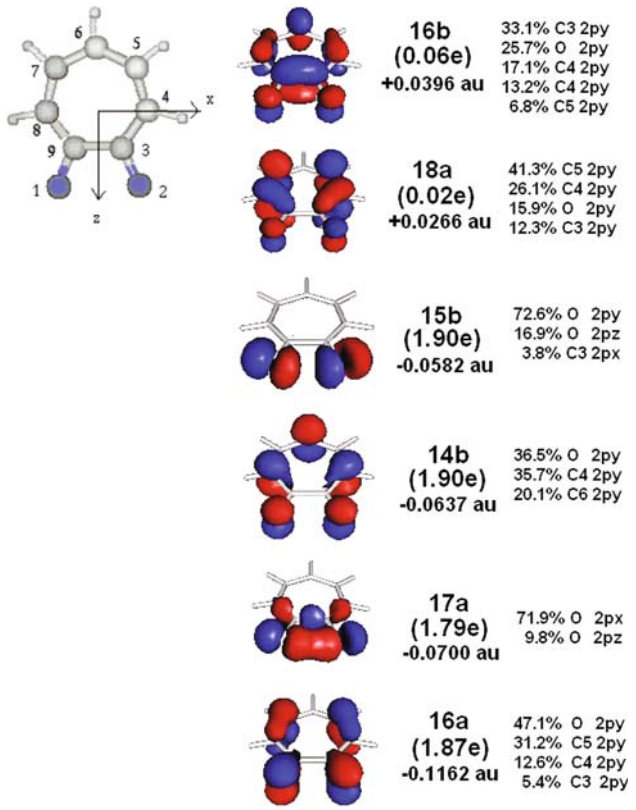

Fig. 5 The tropolonate-localized fragment orbitals mostly involved in the metal–ligand covalent interaction. In the isolated fragment, the 16b and 18a orbitals are virtual orbitals, 15b is the highest in energy occupied molecular orbitals (HOMO). The percentage composition in terms of valence atomic orbitals is reported for each orbital

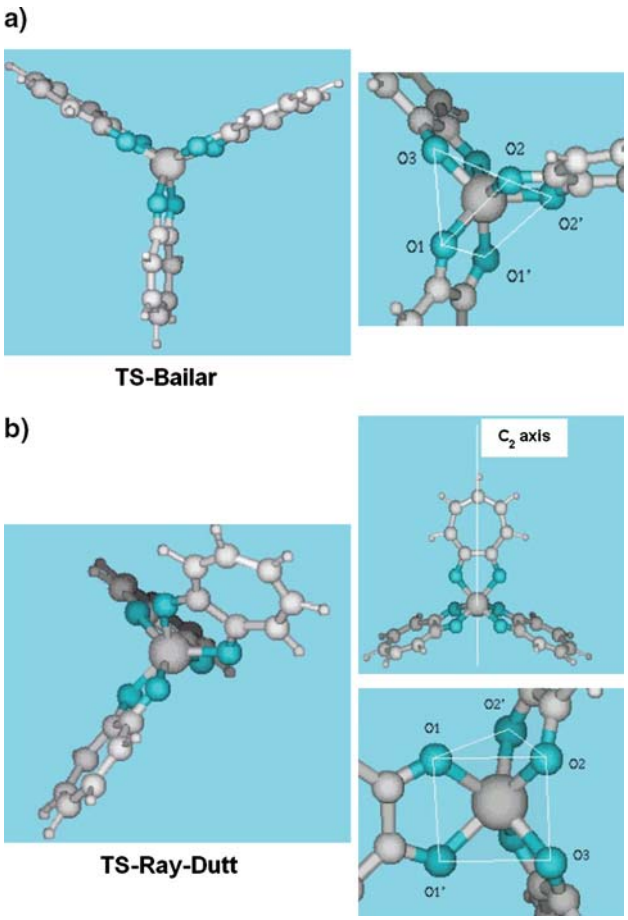

Fig. 6 The Bailar **a** and Ray-Dutt **b** twists transition structures. In the Ray-Dutt transition structures, we can distinguish a chelant along the C_2 rotation. For both the structures, the donor atoms have been labelled for reference in Table 3

still considered associated to a Bailar twist. Such a possibility has been investigated by a study of the PES around the TS-Bailar structure. Starting from lower symmetry structure and moving toward a transition structure point we have always found the same transition structure belonging to the D_{3h} point group symmetry.

Table 3 collects some computed geometrical parameters of the TS-Bailar structure, and its variation in comparison to the minimum-energy structure. It is interesting to note that both the 3-21G(d) and the 6-31G(d) describe the same elongation of the Al–O bond distance. The agreement between the two basis sets is substantially kept for the other geometrical parameters. Not surprisingly, the tropolonate chelant structures appear mostly unaffected by the twist, with a maximum deviation from the minimum point of only 0.004 Å for the C–O bond distance described by the 3-21G(d) basis set (still lower for the 6-31G(d) basis set).

The transition vector of the TS-Bailar structure belongs to the A_1" irreducible representation, thus a displacement along such a vector leads to a lowering of the point symmetry group from D_{3h} to D_3. Thus, the MEP is associated to the D_3 point symmetry, as expected from an ideal Bailar twist process.

According to proposed symmetry rules [40], additional maximum-symmetry reaction paths which invert the AlT_3 chirality can exist which are consistent with a Ray-Dutt twist process. The symmetry point group of a such a structure is C_{2v}. Thus, even in this case, we deal with an achiral transition structure which connects chiral minimum structures. In this case, a displacement along the transition vector should lead to a C_2 point symmetry structure and this is the symmetry of the molecule along the MEP.

All these predictions have been confirmed by our computations. Figure 6 shows the transition structure clearly consistent with a Ray-Dutt twist. Such a structure will be referred to as "TS-Ray-Dutt" in the following and belongs to the C_{2v} symmetry point group, thus it is an achiral structure. The transition vector is of A_2 symmetry, a displacement from the TS-Ray-Dutt structure along the transition vector leads to the predicted C_2 structure on the MEP. From the geometrical parameters listed in Table 3, it can be observed that the Al–O distances of the chelant along the C_2 axis (Al–O_1) are longer than the ones of the other chelants. In comparison

Table 3 Some computed geometrical parameters of the AlT_3 TS-Bailar and TS-Ray-Dutt transition structures in comparison to the minimum structure. Fig. 6 for the labels of the chelant donor atoms

Parameter	B3LYP/3-21G(d) (Å and degrees)	B3LYP/6-31G(d) (Å and degrees)
TS-Bailar		
Al–O	1.932 (+0.033)	1.947 (+0.033)
O1–O1' (Bite)	2.447 (−0.057)	2.467 (−0.045)
O1–O2	2.589 (−0.149)	2.609 (−0.145)
O1–O2'	3.562 (+0.796)	3.591 (+0.777)
O1–Al–O1'	78.6 (−3.9)	78.6 (−3.4)
O1–Al–O2'	134.5 (+41.0)	134.5 (+39.9)
O1–Al–O2	84.2 (−8.0)	84.1 (+7.9)
TS–Ray-Dutt		
Al–O1	1.944 (+0.045)	1.969 (+0.055)
Al–O2	1.917 (+0.018)	1.934 (+0.020)
O1–O1' (Bite)	2.444 (−0.060)	2.459 (−0.053)
O2–O2' (Bite)	2.493 (−0.011)	2.507 (−0.005)
O1–O2	2.582 (−0.156)	2.620 (−0.134)
O1–Al–O1'	77.9 (−4.6)	77.3 (−4.7)
O2–Al–O2'	81.1 (−1.4)	80.8 (−1.2)

to the minimum structure, the Al-O_1 distance is 0.055 Å longer (B3LYP/6-31G(d)), whereas the other Al-O distances are 0.020 Å longer (B3LYP/6-31G(d)). As a consequence, the bite distance of the axial chelant is shorter in comparison to the non-axial chelant. As in the TS-Bailar structure, the chelant structure is only marginally changed in comparison to the minimum structure. The largest computed difference is 0.003 Å for one of the C–O distances in both the used basis sets.

3.3 The likelihood of bond-breaking MEPs in AlT_3

Among the postulated reaction paths, bond-breaking paths can take place that compete with twist paths. Such isomerization processes involve the breaking of one metal–donor bond with consequent formation of 5-coordinated complexes [40]. Gordon and Holm [12] have classified these paths according to the geometry of the transient 5-coordinated structure. Accordingly, we can have paths going through trigonal bipyramidal transient structures (TBP paths) and through square pyramidal transient structures (SP paths). The interested reader is addressed to the suggested bibliography [2,12] for a deeper discussion. In Fig. 7, we report two possible TBP paths which can be named according to the position of the dangling chelant, that is equatorial (TBPeq) or axial (TBPax), plus one of the postulated transient structure among the several SP paths.

We have not been able to find out any of these reaction paths. According to our investigations about the AlT_3 PES, the only reasonable bond-breaking path should be a TBPeq transition structure lying above 39 kcal/mol relative to the minimum structure. As evident in the following, such energies are well higher than the twist paths that have been found. In this sense, according to our findings, the experimentally observed reaction paths should be assigned to the two twist rearrangements whose transition structures have been previously discussed.

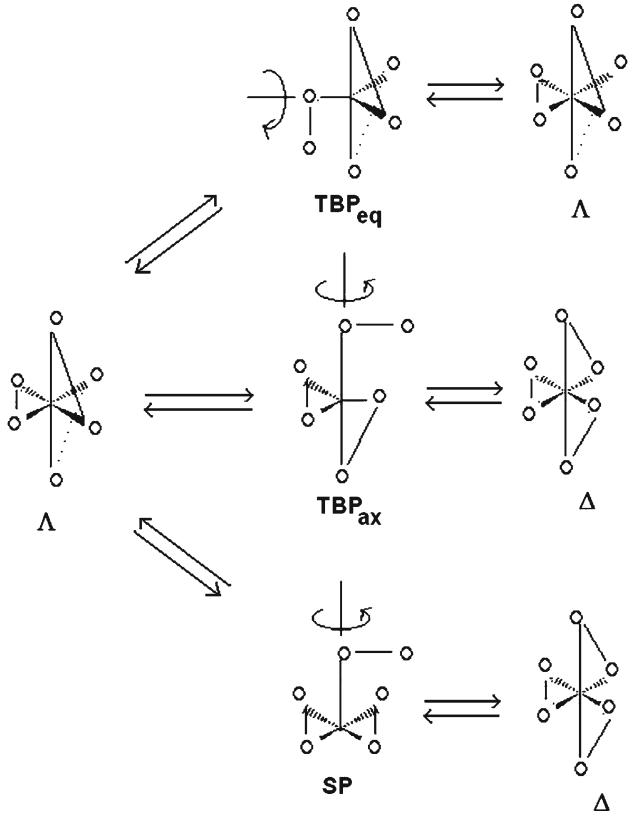

Fig. 7 Possible bond-breaking paths and their effect on the complex isomery in case of tris-chelated complexes with symmetric chelants

3.4 The aluminum complexes with α-C_3H_5-tropolonate and α-C_3H_7-tropolonate chelants

As said above, the reference experimental study for our computations has been performed on Al(α-C_3H_5–T)$_3$ and Al(α-C_3H_7-T)$_3$ [21] (Fig. 2a). The authors have possibly chosen the two hydrocarbon substituents on the tropolonate chelants with the goal of a good balance between the need of asymmetric chelants (for the dynamic NMR study) and the necessity of low perturbation of the coordination sphere (metal–ligand interactions) and isomerization kinetics. A possible way to test the effect of perturbation induced by the substituents is the comparison between the *trans* and *cis* structure energy. Similar energies mean a low perturbation of the AlT_3 coordination sphere.

Table 4 Experimental and computational (ONIOM) results about the *cis*→*trans* equilibrium of Al(α-C_3H_5-T)$_3$ and Al(α-C_3H_7-T)$_3$

Source	ΔH° (kcal/mol)	ΔS° (cal k^{-1}mol^{-1})	ΔG° (kcal/mol)
Al(α-C_3H_5-T)$_3$			
Experimental [21] ($C_2H_2Cl_4$ solution)	-1.7 ± 0.2	-2.7 ± 0.3	-0.9 ± 0.1
Experimental [21] (CH_2Cl_2 solution)	-0.20 ± 0.02	$+2.2 \pm 0.2$	-0.8 ± 0.1
Computational B3LYP/6-31G(d) (vacuum)	0.0	+0.1	−0.1
Computational ONIOM (vacuum)	+0.1	+0.1	+0.1
Al(α-C_3H_7-T)$_3$			
Experimental [21] ($C_2H_2Cl_4$ solution)	0.0 ± 0.5	$+2.9 \pm 0.5$	-0.9 ± 0.5
Computational B3LYP/6-31G(d) (vacuum)	0.0	+0.1	−0.1
Computational ONIOM (vacuum)	0.0	0.0	−0.1

In our computational study, the effects of the substituents on the tropolonate ligands have been included by using the ONIOM approach as detailed in the Sect. 2. This method has been tested by comparison with fully optimised structures at the B3LYP/6-31G(d) level of approximation, and successively it has been applied to the determination of the transition structures.

Table 4 collects some experimental and computational thermodynamic parameters for the *cis* → *trans* equilibrium of the studied complexes. Both the B3LYP/6-31G(d) and the ONIOM results are listed. The two computational methods show a substantial stability equivalence in *cis* and *trans* isomers of Al(α-C_3H_5-T)$_3$ and Al(α-C_3H_7-T)$_3$, confirming the low perturbation of the hydrocarbon substituents on the complex coordination sphere. This result is in very good agreement with the experimental data for Al(α-C_3H_7-T)$_3$. The reported experimental larger stability of the *trans* isomer in terms of Gibbs standard energy seems to be associated to entropic effects. These might be due to solvation effects which are not considered in our computations, and give a possible explanation of the computational error on ΔG°. In the case of Al(α-C_3H_5-T)$_3$, the computations are in relatively worse agreement with experimental data, although they substantially confirm the high similarity between *cis* and *trans* thermodynamic parameters. The fact that ΔH^0 passes from –1.7 ± 0.2 kcal/mol in $C_2H_2Cl_4$ solution to –0.20 ± 0.02 kcal/mol in CH_2Cl_2 solution suggests the relevance of solvation effects in determining the equilibrium position in the case of two isomers of very similar stability. Furthermore, we can underline the good agreement between the full ab initio approach and the ONIOM approach in predicting thermodynamic properties. In this sense, ONIOM computations have been directly applied to the determination of thermodynamic activation parameters of the Bailar and Ray-Dutt processes.

A point to be discussed is the orientation of the substituents on the tropolonate ligands. Figure 8 is a qualitative view of the position of the C_3H_5 and C_3H_7 groups in the complex.

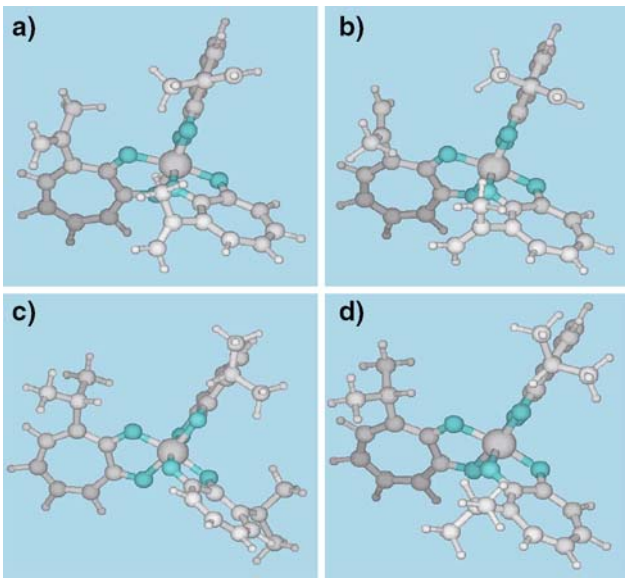

Fig. 8 The computed orientation of the substituents of the tropolonate ligands: **a** C_3H_5 substituent at the B3LYP/6-31G(d) level of approximation; **b** C_3H_5 substituent at the ONIOM level; **c** C_3H_7 substituent at the B3LYP/6-31G(d) level of approximation; **d** C_3H_7 substituent at the ONIOM level

Both ab-initio and ONIOM computations substantially agree in locating the C_3H_5 group in a tilted position in comparison to the tropolonate plane. The dihedral angle between the two plains is about 88 and 62° in ONIOM and B3LYP/6-31G(d) computations, respectively. These values have been observed in all the chelants, both in *cis* and *trans* structures. A closer agreement is found in the description of the C_3H_7 group between the two computational methods (Figs. 8c, 8d).

The fact that the C_3H_5 group is not coplanar with the tropolonate ring was not considered in the experimental work [21]. The authors assumed that such a group is in the plane of the tropolonate chelant. This fact was deduced by the presence of an apparently single methyl NMR signal in the recorded spectra. On the other hand, C_3H_7 groups produce two

Table 5 Experimental results [21] about isomerization kinetics of Al(α-$C_3H_5-T)_3$ and Al(α-C_3H_7-T)$_3$

Process	E_a (kcal/mol)	$\Delta H^{\neq}$ (kcal/mol)	$\Delta G^{\neq}$ (kcal/mol)	$\Delta S^{\neq}$ (cal $k^{-1}mol^{-1}$)
Al(α-$C_3H_5T)_3$				
$T\Delta \rightarrow T\Lambda$ (Bailar)[a]	13.2 ± 1.4	12.6 ± 1.4	14.9 ± 1.2	-7.4 ± 4.8
$C \rightarrow T$[b]	16.9 ± 1.1	16.2 ± 1.0	17.5 ± 1.4	-4.3 ± 3.2
Al(α-$C_3H_7T)_3$				
$C\Delta \rightarrow C\Lambda$(Bailar)[a]	10.5 ± 3.6	10.0 ± 3.6	14.6 ± 5.0	-16 ± 12
$T\Delta \rightarrow T\Lambda$(Bailar)[a]	12.3 ± 2.0	11.7 ± 2.0	14.9 ± 2.8	-11 ± 7
$C \rightarrow T$[a]	25.8 ± 4.0	25.1 ± 4.0	18.7 ± 5.3	$+21 \pm 12$

[a] Measure in $C_2H_2Cl_4$ solution
[b] Measure in CH_2Cl_2 solution

visible methyl signals at low temperatures due to different magnetic environments probed by the two methyl groups in the complex (the two methyl groups are diastereotropic in the complex). The methyl signals in C_3H_5 are clearly broader in comparison to the C_3H_7 ones. All these facts suggest the existence of a fast rotation of the C_3H_5 group that averages the two magnetic environments above and below the tropolonate plane.

Interestingly, according to our computations, the lack of planarity between the C_3H_5 group and the tropolonate ring is already present in the isolated ligand, thus, it is not uniquely induced by steric interactions between the chelants in the complex. We have performed a relaxes PES scan by rotating the C_3H_5 respect to the tropolonate ring in an isolate tropolonate molecule and found an energy barrier of about 3.4 kcal/mol between the two positions of the methyl group across the two sides of the tropolonate plane. In the case of α-C_3H_7-tropolonate ligand, a similar study led to a higher rotational barrier of about 7.9 kcal/mol. This fact could explain the possibility of a clear observation of the two magnetic environments in the case of Al(α-C_3H_7-T)$_3$.

To further describe the influence of the hydrocarbon substituents on the complex coordination sphere, the computed Al–O distances span the 1.905–1.919 Å range in the case of Al(α-C_3H_7-T)$_3$ and the 1.907–1.915 Å range in the case of Al(α-C_3H_5-T)$_3$ at the B3LYP/6-31G(d) level of approximation (1.914 Å in AlT_3). The ONIOM computations led to 1.904–1.918 Å and 1.906–1.920 Å ranges, respectively.

3.5 Comparison with the experimental isomerization kinetics

The reported kinetic study about Al(α-C_3H_5-T)$_3$ and Al(α-C_3H_7-T)$_3$ [20] distinguished low-temperature-induced (low activation) isomerization paths and high-temperature-induced (high activation) isomerization paths. The first ones consist in $\Lambda - \Delta$ chirality inversion without *cis–trans* isomerization. They were assigned to the Bailar twist of the *trans* isomer in Al(α-C_3H_5-T)$_3$. On the other hand, in Al(α-C_3H_7-T)$_3$, the $\Lambda - \Delta$ inversion was observed for both the *cis* and *trans* isomers. The high-temperature processes lead to*cis-trans* isomerization and were not clearly assigned to any reaction path by the authors. Table 5 collects the reported activation parameters. It is interesting to note the presence of a negative activation entropy for the processes assigned to the Bailar twist. This point has been considered a property of twist processes; bond-breaking processes are supposed to be associated to positive and larger activation entropies. Such a result has been found in the case of Al(α-C_3H_5-T)$_3$ and Al(α-C_3H_7-T)$_3$. On the other hand, *cis–trans* isomerizations ($C \rightarrow T$ entry in Table 5) still presents a negative activation entropy in the case of Al(α-C_3H_5-T)$_3$, whereas the activation entropy is reported positive in the case of Al(α-C_3H_7-T)$_3$.

Table 6 lists some computed activation parameters. Both the *ab-initio* computations performed on AlT_3 and the ONIOM computations performed on Al(α-C_3H_7-T)$_3$ agree in assigning the faster isomerization processes to the Bailar twist. The second found isomerization process, the Ray-Dutt twist, is slower. In fact, the computed activation energy (Born–Oppeneimer PES) is 2.2 and 1.7 kcal/mol higher in the case of AlT_3 Ray-Dutt process at the B3LYP/6-31G(d) and B3LYP/6-311G(d,p) levels of approximation, respectively. The activation entropy is more negative in the case of the Bailar twist, with consequent lower (Bailar)–(Ray-Dutt) energy difference in terms of Gibbs energy (1.8 and 1.3 kcal/mol respectively, for the B3LYP/6-31G(d) and B3LYP/6-311G (d,p) computations).

Table 6 also reports the results from computations performed with solvation effects (the PCM model as described in Sect. 2). Solvation does not significantly change the trend in energy stability and activation entropy between the TS-Bailar and TS-Ray-Dutt structures. Also the PBE-based computations (Sect. 2) do not change the trend. This fact suggests the lack of significant functional-induced biases in our computations.

In the case of Al(α-C_3H_7-T)$_3$, the computed activation parameters are in good agreement with AlT_3 at the B3LYP/6-31G(d) level of approximation, as expected from the already observed low influence of the tropolonate substituents on the complex PES.

Table 6 Computational results about isomerization kinetics of Al(α-C_3H_5-T)$_3$ and Al(α-C_3H_7-T)$_3$

TS-structure and method	ΔE_{el} (kcal/mol)	ΔE^0 (kcal/mol)	$\Delta H^{\neq}$ (kcal/mol)	$\Delta G^{\neq}$ (kcal/mol)	$\Delta S^{\neq}$ (cal k^{-1} mol^{-1})
AlT_3					
TS-Bailar B3LYP/6-31G(d)	15.9	15.6	14.4	16.2	−6.0
TS-Ray-Dutt B3LYP/6-31G(d)	18.1	17.8	17.4	18.0	−2.0
TS-Bailar B3LYP/6-311G(d,p)	13.2[a]	12.9[b]	11.7[b]	13.5[b]	−6.0[b]
TS-Ray-Dutt B3LYP/6-311G(d,p)	14.9[a]	14.6[b]	14.2[b]	14.8[b]	−2.0[b]
TS-Bailar PCM B3LYP/6-311G(d,p)	14.4[a]	14.1[c]	12.9[c]	14.7[c]	−6.0[c]
TS-Ray-Dutt PCM B3LYP/6-311G(d,p)	18.2[a]	17.9[c]	17.5[c]	18.1[c]	−2.0[c]
TS-Bailar PBE/6-311G(d,p)	12.9[a]	14.6[b]	14.3[b]	15.3[b]	−9.5[b]
TS-Ray-Dutt PBE/6-311G(d,p)	14.8[a]	16.6[b]	16.2[b]	17.3[b]	−3.7[b]
Al(α-C_3H_7-T)$_3$					
C $\Lambda \rightarrow$ CΔ(Bailar) ONIOM	15.0	14.6	14.3	15.4	−3.4
T$\Lambda \rightarrow$ TΔ(Bailar) ONIOM	15.0	14.6	14.3	15.5	−3.9
C$\Lambda \rightarrow$ TΔ(Ray-Dutt) ONIOM	17.7	17.3	16.9	18.1	−3.9
T$\Lambda \rightarrow$ TΔ(Ray-Dutt) ONIOM	17.6	17.3	16.9	18.2	−4.4

[a] Single point computations with the 6-311G(d,p) basis set on the geometry optimised with the 6-31G(d) basis set
[b] Zero-point energies and thermodynamic corrections are computed with the 6-31G(d) basis set and added to the electronic energies by the 6-311G(d,p) basis set
[c] Zero-point energies and thermodynamic corrections are computed at the B3LYP/6-31G(d) level of approximation without using the PCM solvation models

Hence, we can conclude that the experimentally observed fast processes can be effectively assigned to the Bailar twist. According to the computations, the slow processes have to be assigned to Ray-Dutt twists. In fact, as reported in Fig. 3, the Ray-Dutt twist is capable to induce a *cis–trans* isomerization. Furthermore, as said above, our results suggest a much higher value of the activation energies in bond-breaking paths. Thus, it appears unlikely that bond-breaking processes could be responsible of the observed isomerization processes.

A comparison of Tables 5 and 6 allows to easily verify the experimental–computational agreement in the case of Al(α-C_3H_5-T)$_3$. On the other hand, in the case of Al(α-C_3H_7-T)$_3$, $\Delta - \Lambda$ inversions, the agreement with the computations can be considered equally good. However, for the *cis–trans* isomerizations, the experimental entropic and enthalpic activation parameters do not show a similarly good match. Neither a good agreement can be observed between the experimental data about Al(α-C_3H_7-T)$_3$ and Al(α-$C_3H_5 - T$)$_3$ *cis–trans* isomerizations. On the other hand, the activation Gibbs energy is in line both with the computations and with the Al(α-$C_3H_5 - T$)$_3$ experimental data. In this light, this suggests the possibility that an error in the evaluation of the two contribution to the Gibbs activation energy have been performed in the case of Al(α-C_3H_7-T)$_3$ *cis-trans* isomerizations.

The computed negative activation entropy of twist processes is originated by vibrational contributions to the entropy. The computed vibrational spectra of the Bailar and Ray-Dutt transition structures show that the low-frequency vibrational modes are stiffer in the transition structures than the minimum structure (that is, higher force constants are computed). This is induced by the higher steric hindrance probed by the chelants in the prismatic structure and leads to the reduction of the vibrational "amplitude" in the inner coordination-sphere low-frequency deformation modes. Hence, the vibrational quanta of such vibrations increase with consequent lowering of the vibrational entropy of the prismatic structure.

4 Conclusions

Tris-chelated complexes of aluminum with tropolonate and the studied α-substituted-tropolonate undergo isomerization processes through twist paths. The Bailar twist is the fastest process, shortly followed by the Ray-Dutt twist. Bond breaking paths are excluded as competitive processes. These facts allowed the experimental observation of the Bailar twist at lower temperatures in comparison to *cis–trans* isomerization processes that we associate to the Ray-Dutt twist.

Interestingly, the fact that the Bailar and Ray-Dutt twists show close kinetic constants is in good agreement with the prediction of the Kepert's model. According to this approach, the tropolonate normalised bite of 1.3 would mean competition between Bailar and Ray-Dutt twists.

Both experimental and computational works agree in assigning a negative activation entropy to the twist processes. Such an evidence has been considered a possible way to distinguish twist processes from bond-breaking processes. According to our computations, the cause of this feature is an increase of the low-frequency vibrational quanta in the prismatic transition structures of the twist processes due to the higher steric hindrance between the chelants in such a conformation.

Acknowledgments This work has been supported by the Italian Ministero dell'Istruzione, dell'Università e della Ricerca (MiUR) through PRIN 2005 200503527 grant.

References

1. Eisenberg R, Ibers JA (1966) Inorg Chem 5:411
2. Purcell FP, Kotz JC (1977) Inorganic chemistry, Holt-Saunders International Editions, Philadelphia, Chaps 10 and 14
3. Kepert DL (1977) Prog Inorg Chem 23:1
4. Bailar JC (1958) J Inorg Nucl Chem 5:411
5. Ray P, Dutt TS (1943) J Indian Chem Soc 20:81
6. Rodger A, Johnson BFG (1988) Inorg Chem 27:3061
7. Palazzotto MC, Duffy DJ, Edgar BL, Que L, Pignolet LM (1973) J Am Chem Soc 95:4537
8. Healy PC, Whyte AH (1972) J Chem Soc, Dalton Trans 1163:1163
9. Merlino S (1968) Acta Crystallogr Sec B 24:1441
10. Brennan T, Bernal I (1969) J Phys Chem 73:443
11. Lingafelter EC, Braun RL (1966) J Am Chem Soc 88: 2951–2956
12. Gordon JG, Holm RH (1970) J Am Chem Soc 92:5319
13. Girgis AY, Fay RC (1970) J Am Chem Soc 92:7061
14. Rzepa HS, Cass ME (2006) Inorg Chem 46:8024
15. Dowley P, Garbett K, Gillard RD (1967) Inorg Chim Acta 1:278
16. Gillum WO, Wentworth RF, Childers RF (1970) Inorg Chem 9:1825
17. Kane-Maguire NAP, Hanks TW, Jurs DG, Tollison RM, Heatherington AL, Ritzenthaler LM, McNulty LM, Wilson HM (1995) Inorg Chem 34:1121
18. Fay RC, Piper TS (1964) Inorg Chem 3:348
19. Eaton SS, Eaton GR, Holm RH, Muetterties EL (1973) J Am Chem Soc 95:1116
20. Hutchinson JR, Gordon JG, Holm RH (1971) Inorg Chem 10:1004
21. Eaton SS, Hutchinson JR, Holm RH, Muetterties EL (1972) J Am Chem Soc 94:6411
22. Frisch MJ, Trucks GW, Schlegel HB, Scuseria GE, Robb MA, Cheeseman JR, Montgomery JA Jr, Vreven T, Kudin KN, Burant JC, Millam JM, Iyengar SS, Tomasi J, Barone V, Mennucci B, Cossi M, Scalmani G, Rega N, Petersson GA, Nakatsuji H, Hada M, Ehara M, Toyota K, Fukuda R, Hasegawa J, Ishida M, Nakajima T, Honda Y, Kitao O, Nakai H, Klene M, Li X, Knox JE, Hratchian HP, Cross JB, Adamo C, Jaramillo J, Gomperts R, Stratmann RE, Yazyev O, Austin AJ, Cammi R, Pomelli C, Ochterski JW, Ayala PY, Morokuma K, Voth GA, Salvador P, Dannenberg JJ, Zakrzewski VG, Dapprich S, Daniels AD, Strain MC, Farkas O, Malick DK, Rabuck AD, Raghavachari K, Foresman JB, Ortiz JV, Cui Q, Baboul AG, Clifford S, Cioslowski J, Stefanov BB, Liu G, Liashenko A, Piskorz P, Komaromi I, Martin RL, Fox DJ, Keith T, Al-Laham MA, Peng CY, Nanayakkara A, Challacombe M, Gill PMW, Johnson B, Chen W, Wong MW, Gonzalez C, Pople JA (2003) Gaussian 03, Revision B.05, Gaussian, Pittsburgh
23. Schaftenaar G, Noordik JHJ (2000) Comput.-Aided Mol. Design 14: 123–134 (http://www.cmbi.ru.nl/molden/molden.html)
24. Parr RG, Yang W (1989) Density functional theory of atoms and molecules. Oxford University Press, Clarendon Press, New York/Oxford
25. Becke AD (1993) J Chem Phys 98:5648–5652
26. Perdew JP, Burke K, Ernzerhof M (1996) Phys Rev Lett 77:3865
27. Perdew JP, Burke K, Ernzerhof M (1997) Phys Rev Lett 78:1396
28. Dapprich S, Komáromi I, Byun KS, Morokuma K, Frisch MJ (1999) J Mol Struct (Theochem) 462:1
29. Stewart JJP (1989) J Comp Chem 10:209
30. Stewart JJP (1989) J Comp Chem 10:221
31. Tomasi J, Mennucci B, Cammi R (2005) Chem Rev 105:2999
32. te Velde G, Bickelhaupt FM, Baerends EJ, Fonseca Guerra C, Van Gisbergen SJA, Snijders JG, Ziegler T (2001) J Comput Chem 22:931; http://www.scm.com/Doc/Doc2000/Welcome.html
33. Becke AD (1988) Phys Rev A 38:3098
34. Lee C, Yang W, Parr RG (1988) Phys Rev B 37:785
35. Rodger A, Schipper PE (1986) Chem Phys 107:329
36. Rodger A, Schipper PE (1987) J Phys Chem 91:189
37. Rodger A, Schipper PE (1988) Inorg Chem 27:458
38. Schipper PE (1988) J Phys Chem 92:122
39. Muetterties EL, Guggenberger LJ (1972) J Am Chem Soc 94:8046
40. Amati M, Lelj F (2002) Chem Phys Lett 363:451